Macromolecular Research, Vol. 14, No. 3, pp 318-323 (2006)

Rheological Behavior of Polymer/Layered Silicate Nanocomposites under Uniaxial Extensional Flow

Jun Uk Park, Jeong Lim Kim, Do Hoon Kim†, Kyung Hyun Ahn*, and Seung Jong Lee

School of Chemical Engineering, Seoul National University, Seoul 151-744, Korea

Kwang Soo Cho

Department of Polymer Science, Kyungpook National University, Daegu 702-701, Korea

Received January 10, 2006; Revised March 2, 2006

Abstract: We investigated the rheological behaviors and orientation of three different types of layered silicate composite systems under external flow: microcomposite, intercalated and exfoliated nanocomposites. Rheological measurements under shear and uniaxial extensional flows, two-dimensional, small-angle X-ray scattering and transmission electron microscopy were conducted to investigate the properties, as well as nano- and micro-structural changes, of polymer/layered silicate nanocomposites. The preferred orientation of the silicate layers to the flow direction was observed under uniaxial extensional flow for both intercalated and exfoliated systems, while the strain hardening behavior was observed only in the exfoliated systems. The degree of compatibility between the polymer matrix and clay determined the microstructure of polymer/clay composites, strain hardening behavior and spatial orientation of the clays under extensional flow.

Keywords: nanocomposite, exfoliation, rheology, strain hardening, extensional flow.

Introduction

Polymer/clay nanocomposites have attracted a great deal of interest as an effective way to overcome shortcomings of conventional composites since the synthesis of nylon/clay nanocomposites by in-situ polymerization.[1-4] With a smaller loading content, the silicate layers provide unique properties in polymer performance over conventional fillers. These value-added properties can not be shared by conventional composites and adjusted for practical applications.[5,6] To further exploit the performance of polymer/layered silicate nanocomposites, understanding the rheological properties of these materials is crucial.[7] The viscoelasticity of nanocomposites has been extensively studied to elucidate the changes in polymer dynamics and the influence of the nanoscale structures on the structure-property relationships.[8-13] The general conclusions from these studies indicate that the viscoelastic measurements are powerful methods to probe the underlying structure of nanocomposites because of the high sensitivity to the nanoscale dispersion and the strength of the polymer-inorganic interaction. There are many reports about dynamic rheological properties of polymer/clay nanocomposites in shear flow.[8-14] It is well known that both storage and loss modulus under oscillatory shear flow increase with silicate loading at all frequencies and show non-terminal behavior at low frequencies. In the meanwhile, Okamoto *et al.*[15,16] has investigated the orientation of nanoclays under extensional flow. Spatial orientation of clays in nanocomposites must be an important step to realize composite design for property optimization. Extensional behavior of polymers, which is closely related to the melt strength of polymer, has been recognized as one of the important parameters in many polymer processings such as film blowing, blow molding, and thermoforming. Okamoto and coworkers[15] observed a strong strain-induced hardening behavior of polypropylene/clay nanocomposites under uniaxial extensional flow, which according to their argument originates from the alignment of the silicate layers perpendicular to but not parallel to the flow direction. However, considering the large structural anisotropy of the clay, the perpendicular orientation of the clay to extensional direction is hardly acceptable under such a strong flow compared to shear flow. From the viewpoint of the orientation of layered silicates in polymer nanocomposites, several in-situ techniques have been reported combining rheological characterization with simultaneous structural characterization under shear flow. The rheo-small

*Corresponding Author. E-mail: ahnnet@snu.ac.kr

†Current address: Department of Chemical Engineering, University of Texas, Austin, TX 78721, USA.

angle neutron scattering (SANS) technique was used to investigate shear alignment of hectorite clay platelets suspended in an aqueous solution of poly(ethylene oxide).[17] In-situ X-ray scattering has also been applied to investigate the mechanism of layer separation of PP/clay nanocomposites under electric field.[18] Lele *et al.*[14] investigated flow-induced orientation of the layered silicate-syndiotactic polypropylene nanocomposites on molten state using in-situ rheo-x-ray diffraction technique. Park *et al.*[19] investigated disordering of clay layers in the nylon 6/clay nanocomposites. As the melt strength of a polymer or its derivatives and the orientation of fillers are important issues in polymer processing,[20] it will be meaningful to understand the mechanism of strain hardening behavior for designing new materials as well as processing.

In this study, we investigate the effect of three types of morphology, based on the arrangement of the silicate layers in a polymer matrix, on the rheological properties under shear and uniaxial extensional flow, especially focusing on the strain hardening behavior and flow-induced orientation of layered silicates. The materials include microcomposites (where clay plays a role as a conventional inorganic filler), intercalated and exfoliated nanocomposites. Rheological measurements, X-ray diffraction (XRD), two-dimensional small-angle X-ray scattering (2D SAXS) and transmission electron microscopy (TEM) have been used to investigate the material properties as well as nano and micro-structural changes of polymer layered silicate nanocomposites.

Experimental

Preparation of Polymer/Clay Composites. Three types of composites were prepared by mixing polypropylene (PP), maleic anhydride modified polypropylene (MAPP) and polystyrene (PS) with clays. To produce exfoliated nanocomposite systems, PP and organically modified montmorillonite, Cloisite20A (C20A), were mixed with 30 wt% of MAPP, which is abbreviated as PP/MAPP/C20A. PP and MAPP are miscible to each other. So, MAPP was used as a compatibilizer to fabricate PP based exfoliated nanocompoistes and no evidence for phase separation was observed in this study. The other materials are named in the same manner. MAPP and C20A were mixed to produce the exfoliated system as well. PS and C20A were mixed as an intercalated nanocomposite, and PP and natural montmorillonite, Cloisite Na^+ (CNa^+), were mixed with 30 wt% of MAPP to produce phase-separated microcomposite system. The weight fraction of clay was fixed at 5 wt% in all cases. The properties of polymers and clays are listed in Table I. Melt compounding of polymer/clay nanocomposites was carried out in an intensive internal HAAKE mixer (Rheocord 90). The rotor speed was 50 rpm and mixing time was 20 min after clay feeding at 170 °C for PP systems and 200 °C for PS system, respectively. The clay and polymer samples were dried in a vacuum oven at 80 °C for 24 hrs prior to compounding.

Characterization of Polymer/Clay Nanocomposites. XRD measurements (Figure 1) were performed to investigate the characteristic peak of composites using a Rigaku D/AMX-IIIC X-ray diffractometer with Cu-Kα radiation (λ= 1.5405 Å). PP/MAPP/CNa^+ composite (microcomposite system) did not show any change in the characteristic peak compared to neat CNa^+ at 2θ value of 7.54° corresponding to a basal spacing of 11.7 Å (not shown here). They are just immiscible microcomposites even if MAPP was used,

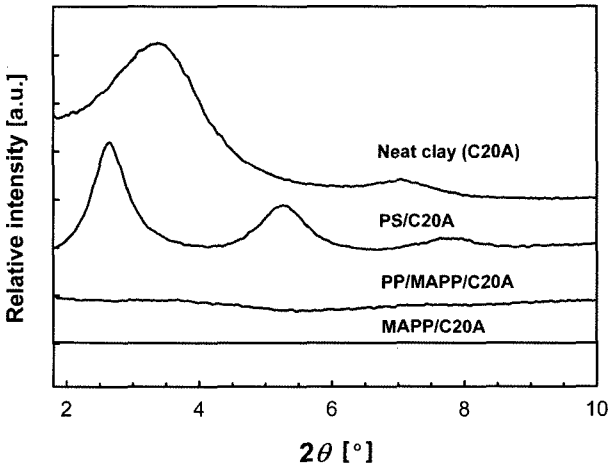

Figure 1. X-ray diffraction patterns for neat clay, polypropylene based composites and polystyrene based composites.

Table I. The Properties of Polymers and Clays

Materials	Grade	Properties
Polypropylene	HP562T (Poly-mirae Corp.)	(M.I.) 60 g/10 min at 230 °C
Polystyrene	GPPS HF-2660 (Samsung Cheil Industries Inc.)	(M.I.) 7.3 g/10 min at 210 °C
Maleic Anhydride Polypropylene	Polybond® 3150 (Uniroyal Chemicals)	(M.I.) 50 g/10 min at 230 °C 0.5 wt% MA Included
Clays	Cloisite® Na^+ Cloisite® 20A (Southern Clay Products Inc.)	Natural Clay Dimethyl Hydrogenated-tallow Ammonium

because hydrophilic clay does not have any compatibility with hydrophobic polymer chains. The XRD curve of PS/C20A composite shows a shift of d_{001} peak to lower 2θ value from 3.37 to 2.71° with a narrow distribution, corresponding to basal spacing of 26.1 and 32.6 Å, repectively, indicating the typical intercalated characteristic. In polypropylene based nanocomposites such as PP/MAPP/C20A and MAPP/C20A, the characteristic peaks disappear after melt compounding indicating the formation of exfoliated nanostructure.

Dynamic oscillatory shear measurements were performed on rheometrics mechanical spectrometer (RMS) 800 using parallel plate geometry with 25 mm diameter plates and 1 mm gap. The setting temperature was 170 °C for PP based system and 200 °C for PS based system. The range of angular frequency was from 10^{-1} to 10^{2} rad/s with a strain of 10% (PP) and 5% (PS), which are in the linear region. All experiments were performed under a nitrogen gas flow to minimize oxidative degradation of the materials.

Transient extensional viscosity was measured using a Meissner-type elongational rheometer (commercialized as RME from Rheometric Scientific). Uniaxial extension was applied at 170 °C for PP and 160 °C for PS, respectively to examine whether the polymer layered silicate composites show strain hardening or not. Samples of 55 mm (length)× 7 mm (width)×1.5 mm (height) were deformed by four fixed rotary clamps while supported by inert gas flow.

Samples have been taken after extensional measurements by rapid quenching to investigate the microstrutural changes of the composites by 2D SAXS and TEM analysis. SAXS measurements were performed using a Bruker AXS (Nanostar, Germany), whose X-ray source is Cu and the maximum generator power is 3 kW. Scattering was obtained over 2θ range of 0.5-12° and beam size of 0.8 mmϕ. TEM investigation was conducted using Jeol JEM-2000EXII at an acceleration voltage of 200 KV to observe how the layered silicates are dispersed in the polymer matrix.

Results and Discussion

Rheological measurements are known to give a good information on the three-dimensional superstructure of silicate layers in nanoscale and mesoscale because of its sensitivity to the microstructural change of nanocomposites.[7-14] The storage modulus data of polypropylene based composites are shown in Figure 2(a). At high frequencies, the responses of the PP/MAPP/C20A and MAPP/C20A nanocomposites are dominated by the matrix PP and MAPP respectively, while its solid-like response is strongly influenced by the presence of the exfoliated layered silicates at lower frequencies. On the other hand, PP/MAPP/CNa^{+} microcomposite does not show significant improvement in the rheological properties regardless of the use of compatibilizer because strong hydrophilicity of natural clay does not have any compatibility with the hydrophobic polymers such as PP and MAPP used in this study. In the case of intercalated nanocomposites, PS/C20A shows a slight non-terminal behavior at low frequencies as shown in Figure 2(b). The results of rheological measurements under shear flow indicate that the difference in compatibility between the clay and the matrix polymer induces different structures of prepared composites. The strongest compatibility produces exfoliated structure (PP/MAPP/C20A, MAPP/C20A) and the intermediate one does intercalated structure (PS/C20A) and the weakest one does conventional microcomposite (PP/MAPP/CNa^{+}).

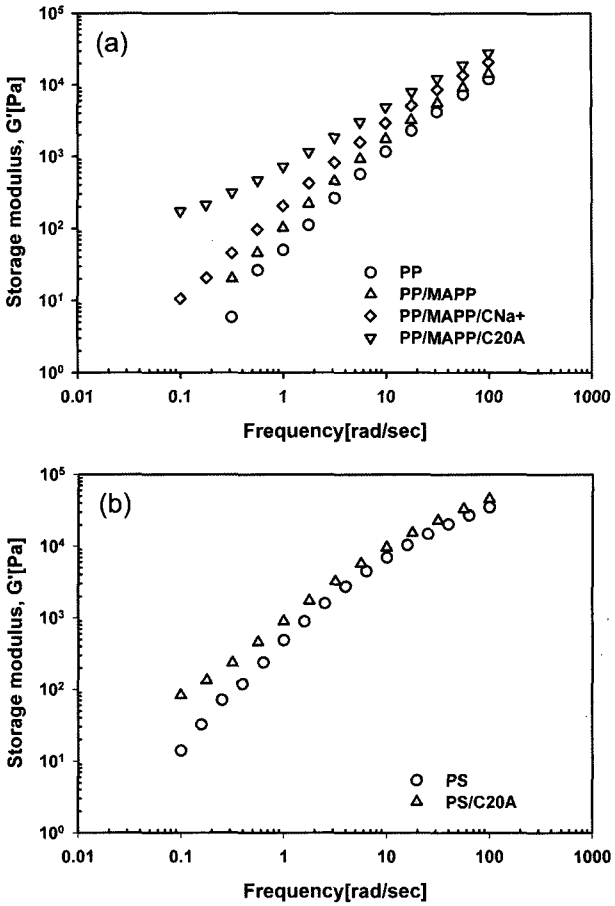

Figure 2. The results of frequency sweep tests: measured at 170 °C for polypropylene based composites (a) and at 200 °C for polystyrene based composites (b).

Figure 3(a) shows transient extensional viscosity data for PP/MAPP/C20A and MAPP/C20A nanocomposites at different extension rates. It is observed that the exfoliated PP/MAPP/C20A and MAPP/C20A nanocomposites show strain hardening behavior under uniaxial extensional flow field. The strain hardening is generally considered as a dramatic increase of extensional viscosity from its zero-rate envelope. In the early stage, the extensional viscosities of PP/MAPP/C20A and MAPP/C20A nanocomposites gradually increase

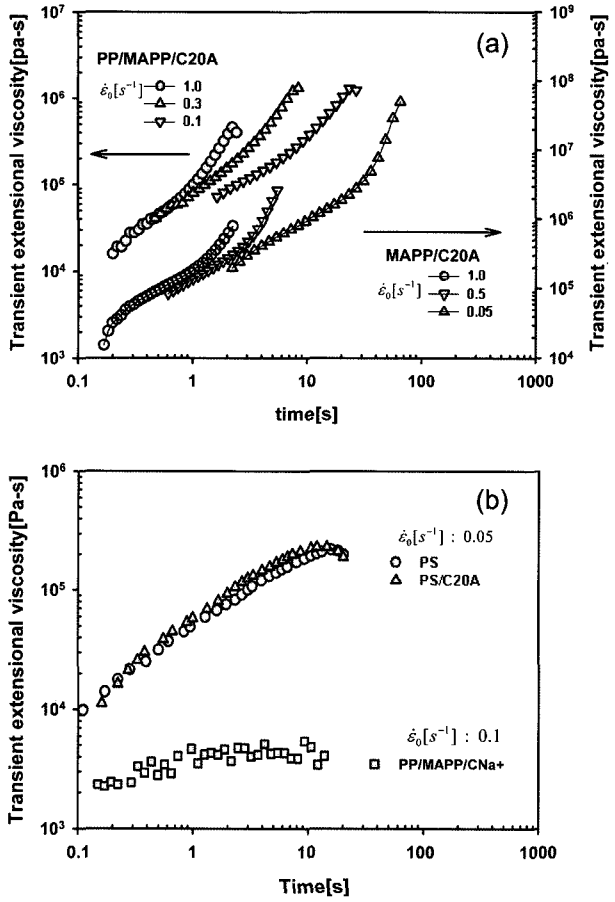

Figure 3. Transient elongational viscosity under uniaxial extensional flow: (a) exfoliated polypropylene based nanocomposites at 170 °C; (b) intercalated polystyrene based nanocomposite and immiscible polypropylene based microcomposite at 160 °C.

along the zero-rate envelope at all extension rates. After a critical strain (strain rate multiplied by time), we can observe an uprising of the extensional viscosity and the break up of specimen at the end. On the other hand, phase-separated microcomposites (PP/MAPP/CNa^+) and intercalated nanocomposites (PS/C20A) do not show any strain hardening behavior as shown in Figure 3(b). Since the exfoliation structure of clay implies a good compatibility and large contact area between layered silicates and polymer matrix, the strain hardening behavior results from such a favorable interfacial nature. It is also noticed that the strain hardening behavior of MAPP/C20A is more pronounced than that of PP/MAPP/C20A, because the former has more polar maleic anhydride groups, which have strong compatibility with organoclays. In addition, the extended Trouton rule, $3\eta_0(\dot{\gamma}_0, t) \cong \eta_E(\dot{\varepsilon}_0, t)$, does not work for both PP/MAPP/C20A and MAPP/C20A nanocomposites, as opposed to ordinary polymer melts.

Figure 4 shows the results of 2D SAXS images of microcomposites (a), intercalated (b) and exfoliated (c,d) nanocomposites under uniaxial extensional flow. All systems show random orientation at the end of the specimen, where it is not stretched. But for the extended specimen, 2D SAXS images of the exfoliated nanocomposites such as PP/MAPP/C20A (c) and MAPP/C20A (d) show two distinctive strings that indicate parallel orientation of the silicate layers along the stretching direction. The intercalated PS/C20A system shows the less orientation parallel to the stretching direction than the exfoliated system. On the other hand, microcomposites such as PP/MAPP/CNa^+ or MAPP/CNa^+ do not show a preferred orientation of the layered silicates in 2D SAXS images (a). If an affine deformation is assumed, it is generally acceptable to observe such an orientation because the uniaxial extensional flow causes the strong streamline parallel to the flow direction and as a result, the silicate layers with high aspect ratio need to preferentially align parallel to the stretching direction. However, in the microcomposite system, it is hard to apply the affine deformation due to the very weak compatibility between the clay and matrix polymer. Less orientation in intercalated system is also the result from weaker compatibility than the exfoliated system.

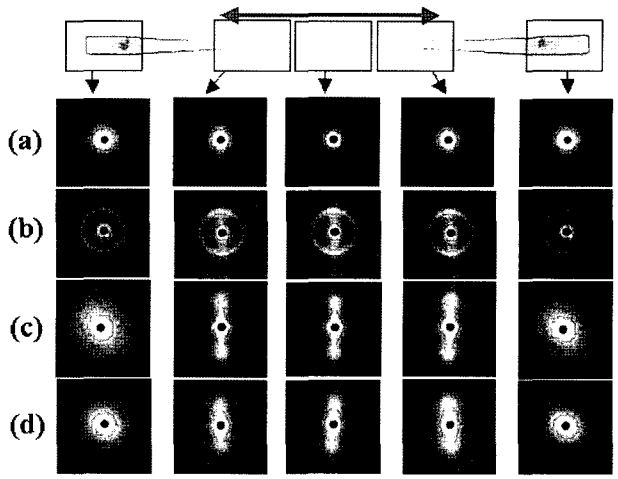

Figure 4. The 2D small-angle X-ray scattering images after uniaxial extensional stretching (arrow indicates stretching direction): (a) PP/MAPP/CNa^+, (b) PS/C20A, (c) PP/MAPP/C20A, and (d) MAPP/C20A.

Figure 5(a) and (b) show the dispersion state of silicate layers within polypropylene matrix before elongational measurements. In both cases, the silicate layers are dispersed homogeneously and randomly throughout the polymer matrix. After stretching, the orientation of silicate layers along the flow direction is clearly observed in both exfoliated cases of PP/MAPP/C20A and MAPP/C20A as shown in Figure 5(c) and (d). Randomly dispersed silicate layers are preferentially oriented along the stretching direction by the extensional flow only in the exfoliated nanocomposites because of the realization of affine deformation arising from the good compatibility between the clay and PP matrix.

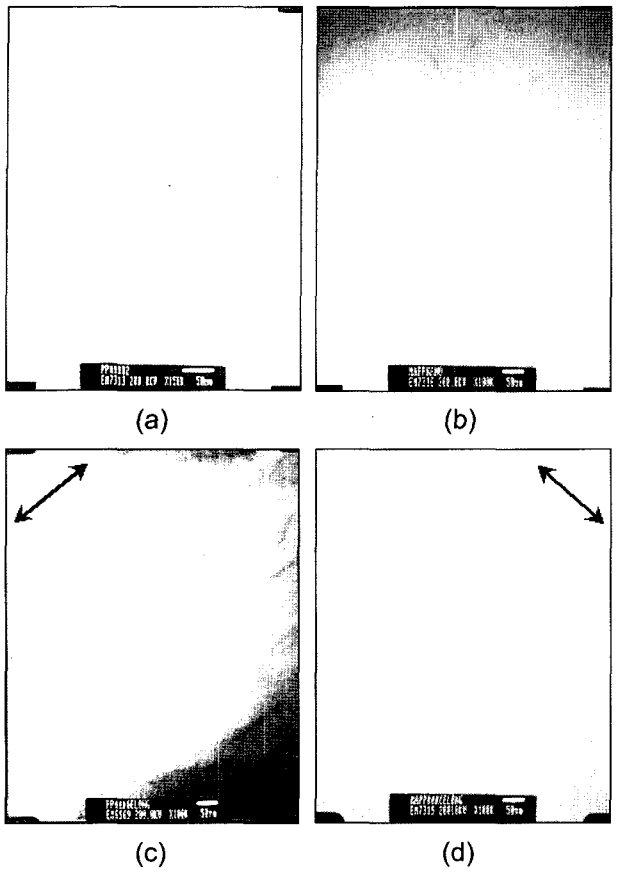

Figure 5. TEM photographs before (a, b) and after (c, d) extensional stretching (arrows indicate stretching direction): PP/MAPP/C20A (a, c) and MAPP/C20A (b, d).

Even though the intercalated system shows a weak orientation similar to the exfoliated system, it does not show any strain hardening behavior unlike the exfoliated system.

The degree of compatibility between the polymer and clay determines the microstructure of polymer/clay composites, exfoliated or intercalated or conventional microcomposites. The phase-separated microcomposite with no compatibility shows neither the strain hardening behavior nor morphological change under the uniaxial extentional flow, while the exfoliated system induced by the strong compatibility shows both the strain hardening behavior and the clay alignment along the flow direction under uniaxial extensional flow. Therefore, generally assumed affine deformation in multiphase systems should be carefully considered according to the interfacial compatibility. Even if the intermediate compatibility in the intercalated system leads to slight orientation of the clays, it does not give rise to the strain hardening behavior.

Conclusions

We prepared polymer/clay composites with three different morphologies and observed preferred orientation of the silicate layers to the flow direction under uniaxial extensional flow for both intercalated and exfoliated systems, while strain hardening behavior was observed only for the exfoliated systems. Although further quantitative analysis is still necessary, the degree of compatibility between the polymer matrix and clay must be a key factor to determine the microstructure of polymer/clay composites, strain hardening behavior and spatial orientation of the clay under extensional flow. Spatial arrangement of the clay and strain hardening behavior has been crucial issues toward the realization of effective composites design and processing for property optimization in polymer/clay nanocompoistes. This research, focusing on the interrelation among the microstructure of composites, strain hardening behavior and alignment of the clay will provide an idea for better design of polymer/clay nanocomposites for potential application.

Acknowledgements. The authors wish to acknowledge the Korea Energy Management Corporation (KEMCO) for the financial support through the Project No. 2005-R-NM01-P-01-2-400-2005.

References

(1) E. P. Giannelis, *Adv. Mater.*, **8**, 29 (1996).
(2) P. C. LeBaron, Z. Wang, and T. J. Pinnavaia, *Appl. Clay Sci.*, **15**, 11 (1999).
(3) M. Alexandre and P. Dubois, *Mater. Sci. Eng.*, **28**, 1 (2000).
(4) J. Collister, in *Polymer Nanocomposites: Synthesis, Characterization, and Modeling*, R. A. Vaia and R. Krishnamoorti, Eds., Oxford Univ. Press, London, 2002, Ch.2.
(5) P. B. Messersmith and E. P. Giannelis, *J. Polym. Sci.; Part A: Polym. Chem.*, **33**, 1047 (1995).
(6) D. Porter, E. Metcalfe, and M. J. K. Thomas, *Fire Mater.*, **24**, 45 (2000).
(7) R. Krishnamoorti and K. Yurekli, *Curr. Opi. Colloid & Interface Sci.*, **6**, 464 (2001).
(8) G. Galgali, C. Ramesh, and A. Lele, *Macromolecules*, **34**, 852 (2001).
(9) R. Krishnamoorti and E. P. Giannelis, *Langmuir*, **17**, 1448 (2001).
(10) Y. T. Lim and O. O. Park, *Macromol. Rapid Comm.*, **21**, 231 (2000).
(11) P. Reichert, B. Hoffmann, T. Bock, R. Thomann, R. Mülhaupt, and C. Friedrich, *Macromol. Rapid Comm.*, **22**, 519 (2001).
(12) J. Ren, A. S. Silva, and R. Krishnamoorti, *Macromolecules*, **33**, 3739 (2000).
(13) M. J. Solomon, A. S. Almusallam, K. F. Seefeldt, A. Somwangthanaroj, and P. Varadan, *Macromolecules*, **34**, 1864 (2001).
(14) A. Lele, M. Mackley, G. Gagali, and C. Ramesh, *J. Rheolgy*, **46**, 1091 (2002).
(15) M. Okamoto, P. H. Nam, P. Maiti, T. Kotaka, N. Hasegawa, and A. Usuki, *Nano Letters*, **1**, 295 (2001).

(16) M. Okamoto, P. H. Nam, P. Maiti, T. Kotaka, T. Nakayama, M. Takada, M. Ohsima, A. Usuki, N. Hasegawa, and H. Okamoto, *Nano Letters,* **1**, 503 (2001).
(17) G. Schmidt, A. I. Nakatani, P. D. Butler, A. Karim, and C. C. Han, *Macromolecules,* **33**, 7219 (2000).
(18) D. H. Kim, J. U. Park, K. H.Ahn, and S. J. Lee, *Macromol. Rapid Commun.*, **24**, 388 (2003).
(19) J. H. Park, W. N. Kim, H. Kye, S. S. Lee, M. Park, J. Kim and S. Lim, *Macromol. Res.*, **13**, 367 (2005).
(20) J. S. Hong, K. H. Ahn, and S. J. Lee, *Korea-Australia Rheology Journal*, **16**, 213 (2004).